Coupled-Channels Model of Self-Consistent Regge Trajectories*

L. CANESCHI† AND A. PIGNOTTI
University of California, Santa Barbara, California 93106
(Received 3 February 1969)

A model in which a vacuum P and a meson M Regge trajectory are present is studied in the framework of the multiperipheral bootstrap. Simultaneous self-consistency is imposed on the intercepts and slopes of both trajectories. In this model the P slope tends to be larger than the M slope, and if the P intercept at $t=0$ is close to 1, the P exchange does not give rise to strong effects.

I. INTRODUCTION

IN a recent paper,[1] we carried out to some extent the multiperipheral bootstrap scheme.[2] The starting point in this approach is the assumption that multiple exchange of an (input) average meson Regge pole M gives a reasonable description of the production amplitude. Through the unitarity sum, and using the integral equation technique suggested by Chew, Goldberger, and Low,[3] and independently by Halliday,[4] an (output) Regge behavior is obtained for the imaginary part of the two-body amplitude. In I, we constrained the input and output intercepts and slopes of the M trajectory to be equal at $t=0$, and obtained a solution with only one degree of freedom. We also showed that the same dynamical mechanism, i.e., multiple M exchange, can be used to generate the Pomeranchuk pole P.

It is clear that the next step toward achieving a complete self-consistent solution is to include also P exchange, and simultaneously enforce self-consistency for the intercepts and slopes of the M and P trajectories. This is done in the present paper. Again we find a solution in which there is some freedom, corresponding to the various internal coupling constants[5] involved, for which a self-consistent determination has not yet been attempted. This freedom enables us to study the limiting cases in which M or P exchange dominates, and various correlations such as between the P intercept and the internal coupling of the P pole. In particular, we find that the ratio of the P to the M slope is not correlated to the smallness of the internal P coupling, and that the M exchange dominates if the P intercept is close to 1.

II. MULTICHANNEL FORMALISM

In order to introduce simultaneous P and M exchanges, we have to extend the formalism used in I to the multichannel case. Each channel is labeled by a pair of indices ij corresponding to the pair of Regge poles that can be exchanged at a given stage in the ladder of Fig. 1. Following the procedure and notation used in I, with the addition of channel indices, we obtain for the imaginary part of the two-body amplitude

$$\mathrm{Im}A(Q,k_0,k_0')=\sum_{ij}\int d^4k\, B^{ij}(Q,k_0,k,k_0')G^i((Q-k)^2)\times G^j((Q+k)^2)\delta((k'_0-k)^2-m^2), \quad (2.1)$$

where G^i is the residue of the ith Regge pole at an external vertex and m is the mass of the external particle. The function $B^{ij}(Q,k_0,k,k_0')$ satisfies the integral equation

$$B^{i'j'}(Q,k_0,k',k'')=B_0{}^{i'j'}(Q,k_0,k',k'')+\int d^4k\, B^{ij}(Q,k_0,k,k')K^{ij,i'j'}(Q,k,k',k''). \quad (2.2)$$

The inhomogeneous term in this equation is

$$B_0{}^{i'j'}(Q,k_0,k',k'')=G^{i'}((Q-k')^2)G^{j'}((Q+k')^2)\times\delta((k'-k_0)^2-m^2)R^{i'j'}(Q,k_0,k',k''), \quad (2.3)$$

where R^{ij} is a product of Regge propagators and depends on the input trajectories α_i and α_j,

$$R^{i'j'}(Q,k,k',k'')=[(k''-k)^2/s_0]^{\alpha_{i'}((Q-k')^2)+\alpha_{j'}((Q+k')^2)}\times S^{i'j'}((Q-k')^2,(Q+k')^2). \quad (2.4)$$

Here, $S^{i'j'}$ is the Regge phase associated with the

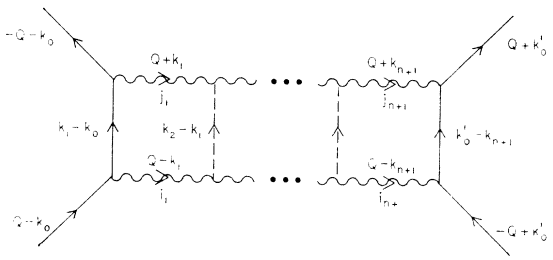

FIG. 1. Unitarity diagram for the n-particle production contribution to ImA.

* Work supported in part by the National Science Foundation.
† Fulbright Fellow.
[1] L. Caneschi and A. Pignotti, Phys. Rev. **180**, 1525 (1969), referred to as I.
[2] G. F. Chew and A. Pignotti, Phys. Rev. **176**, 2112 (1968).
[3] G. F. Chew, M. L. Goldberger, and F. Low, Phys. Rev. Letters **22**, 208 (1969).
[4] I. G. Halliday, Imperial College Report No. ICTP/67/36, 1968 (unpublished).
[5] By "internal coupling constant" we mean the one associated to a vertex at which two Regge poles and a physical particle interact.

signature factor:

$$S^{i'j'}((Q-k')^2,(Q+k')^2)=\exp\{-\tfrac{1}{2}i\pi[\alpha_{i'}((Q-k')^2)-\alpha_{j'}((Q+k')^2)-\tfrac{1}{2}(\sigma^{i'}-\sigma^{j'})]\}, \quad (2.5)$$

where σ^i denotes the signature of the ith Regge pole. The kernel of the equation is

$$K^{ij,i'j'}(Q,k,k',k'')=8g^{ii'}g^{jj'}\psi^i((Q-k)^2)\psi^j((Q+k)^2)\times\psi^{i'}((Q-k')^2)\psi^{j'}((Q+k')^2)\times\delta((k'-k)^2-\mu^2)R^{i'j'}(Q,k,k',k''), \quad (2.6)$$

where μ is the mass of the produced particles, and we have assumed a factorized form $g^{ii'}\psi^i\psi^{i'}$ for the residue at an internal vertex. The functions ψ^i are normalized as in I:

$$\int_{-\infty}^{0}[\psi^i(t)]^4dt=1.$$

We also use linear trajectories, i.e., $\alpha_i(t)=\alpha_i+\alpha_i't$. Equations (2.1)–(2.6) are the generalizations of Eqs. (2.16), (2.15), (2.12), (2.7), (2.8), and (2.14) of I. Again, we solve the integral equation (2.2) for B in terms of its Mellin transform, the singularities of which determine the high-energy behavior of $\mathrm{Im}A$. This is of the Regge type and defines the output trajectory.

We start by expressing the integration in Eq. (2.2) in the form of an integration over a two-body phase space and over the invariant mass squared s of one of the intermediate "particles." Figure 2 shows this pseudo-two-body intermediate state, and defines the invariants used. The most convenient frame for performing the integration is a c.m. frame in which the combination $\alpha_i't+\alpha_j'\tau$ depends only on the polar angle θ but not on the azimuthal angle φ, to first order in Q^2. In this frame we have

$$\alpha_i't+\alpha_j'\tau=\alpha_+'(2\bar{t}+\epsilon r_{ij})$$

and (2.7)

$$\alpha_i't-\alpha_j'\tau=\alpha_+'\delta r_{ij}+\alpha_-'(2\bar{t}-\epsilon r_{ij}),$$

where

$$\alpha_\pm'=\tfrac{1}{2}(\alpha_i'\pm\alpha_j'),\quad r_{ij}=1-(\alpha_-'/\alpha_+')^2,\quad \bar{t}=-\tfrac{1}{2}(s'-s)(1-\cos\theta), \quad (2.8)$$

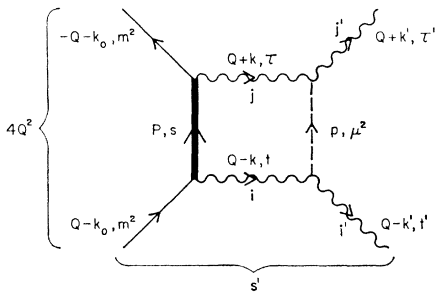

FIG. 2. Definition of variables and channel indices used in the integral equation.

and, for small Q^2,

$$\epsilon\approx 2Q^2(s'-s)/s',\qquad \delta\approx -4[(s'-s)/s']^{1/2}(\bar{t}Q^2)^{1/2}\sin\varphi. \quad (2.9)$$

The approximation

$$(k''-k)^2/s_0\approx(k''-k_0)^2/(k'-k_0)^2 \quad (2.10)$$

again provides an important simplification, after which it is possible to obtain a solution for the integral equation, in analogy to Eq. (3.10) of I. To minimize the number of parameters, we assume a channel-independent[6] exponential parametrization of the vertex functions $\psi^i(t)$ and $G^i(t)$, i.e.,

$$\psi^i(t)=(\sqrt[4]{a})e^{at/4},\qquad G^i(t)=G^i(\sqrt[4]{a})e^{at/4}. \quad (2.11)$$

We point out that the output trajectories are independent of the external residues $G^i(t)$. The solution of the integral equation is

$$B^{i'j'}(Q^2,t',\tau',s',s'')=(s''/s')^{\alpha_{i'}(t')+\alpha_{j'}(\tau')}S^{i'j'}(t',\tau')(\sqrt{a})e^{a(t'+\tau')/4}\times[g^{ii'}g^{jj'}b^{ij}(Q^2,s'/m^2)+G^{i'}G^{j'}\delta(s'-m^2)], \quad (2.12)$$

where summation over repeated indices is implied, and where $b^{ij}(Q^2,x)$ is expressed in terms of its Mellin transform $\tilde{b}^{ij}(Q^2,\beta)$:

$$b^{ij}(Q^2,x)=\frac{1}{2\pi i}\int_{C-i\infty}^{C+i\infty}\tilde{b}^{ij}(Q^2,\beta)x^\beta d\beta. \quad (2.13)$$

The functions $\tilde{b}^{ij}(Q^2,\beta)$ are solutions of a linear algebraic system of equations and can be written

$$\tilde{b}^{i'j'}(Q^2,\beta)=(G^iG^j/m^2)\sigma^{ij}\bar{U}^{ij}(\beta,Q^2)\times[D^{-1}(\beta,Q^2)]^{ij,i'j'}, \quad (2.14)$$

with

$$D^{ij,i'j'}(\beta,Q^2)=\delta_{ij,i'j'}-g^{ii'}g^{jj'}\sigma^{i'j'}\bar{U}^{i'j'}(\beta,Q^2). \quad (2.15)$$

The factor σ^{ij} contains the phase caused by a possible difference of intercepts and signatures of the poles i and j, namely,

$$\sigma^{ij}=\exp\{-\tfrac{1}{2}i\pi[\alpha_i-\alpha_j-\tfrac{1}{2}(\sigma^i-\sigma^j)]\}. \quad (2.16)$$

The functions $\bar{U}^{ij}$ are given by

$$\bar{U}^{ij}(\beta,Q^2)=u^{ij}(\beta,Q^2)-u^{ij}(\beta+1,Q^2)+u^{ij}(\beta+1,0), \quad (2.17)$$

with

$$u^{ij}(\beta,Q^2)=v^{ij}(\beta,Q^2)\left\{1+aQ^2\left[2-r_{ij}-i\pi r_{ij}\frac{\alpha_-'}{a}-\frac{a}{2\alpha_+'}\left(\pi r_{ij}\frac{\alpha_+'}{a}-i\frac{\alpha_-'}{\alpha_+'}\right)^2\left(\beta-\alpha_i-\alpha_j+1\right)\right]\right\}. \quad (2.18)$$

[6] We can solve the integral equation also with parameters a^i that depend on which pole is exchanged. However, we conclude in this paper that M exchange dominates, and therefore the choice of a value of a^P different from a^M is unlikely to produce significant changes in the results.

Here, $v^{ij}(\beta,Q^2)$ are Hilbert transforms of the vertex functions, and can be written in terms of the confluent hypergeometric function Ψ:

$$v^{ij}(\beta,Q^2)=\frac{a}{2\alpha_+'}\int_{-\infty}^{0}\frac{e^{y'}}{y^{ij}-y'}dy'=\frac{a}{2\alpha_+'}\Psi(1,1,y^{ij}), \quad (2.19)$$

with

$$y^{ij}=\left(\frac{a}{2\alpha_+'}+i\tfrac{1}{2}\pi\frac{\alpha_-'}{\alpha_+'}\right)(\beta-\alpha_i-\alpha_j+1-2Q^2r_{ij}\alpha_+'). \quad (2.20)$$

The high-energy behavior of $\mathrm{Im}A$ is controlled by the singularities of $\tilde{b}(Q^2,\beta)$, and the leading pole originates from a zero of the determinant of the matrix $D^{ij,i'j'}$. Note that this matrix is Hermitian for β real and larger than the highest branch point. At $Q^2=0$, this is located at $\beta=\max(\alpha_i+\alpha_j-1)$.

III. SIMULTANEOUS POMERANCHUK AND MESON SELF-CONSISTENCY

We use the formalism developed in Sec. II in a model in which only two trajectories M and P are present, and combined P and M exchanges generate output P and M poles. We assign positive signature to both the P and the M poles, but similar results are obtained with the opposite choice for the M signature. We consider ladder unitarity diagrams built up by iteration of the basic "interactions" of Fig. 3, where the relevant coupling constants are defined. Therefore, two coupled channels, MM and PP, contribute to the vacuum-exchange amplitude, and three channels, PM, MP, and MM, to the amplitude for M exchange. The coefficients C_i in Fig. 3 follow from projection of the diagrams on states of given t-channel quantum numbers. We call them crossing coefficients, and they depend on the internal quantum numbers assumed for the M pole and the on-shell particle represented by a dashed line in Fig. 3. Because they are related to Clebsch-Gordan coefficients, they can vary within a limited range.

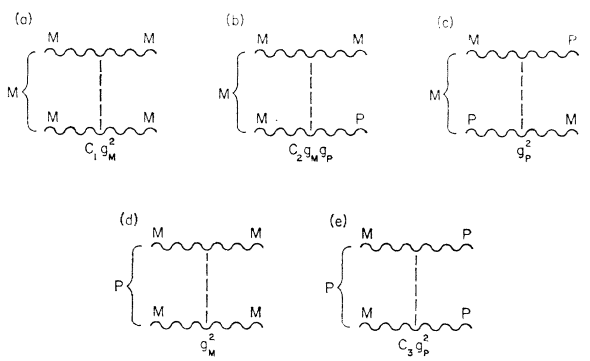

FIG. 3. Interactions considered and definitions of coupling constants and crossing coefficients. The symbols M and P at the left of each diagram stand for the t-channel quantum numbers over which the diagram has been projected.

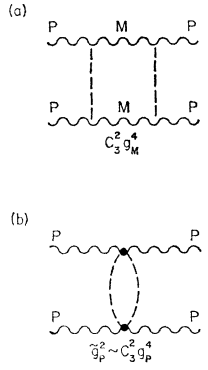

FIG. 4. (a) Diagram for P generation at $g_M=0$. (b) Equivalent PP interaction.

The output P pole originates from the zero of the determinant

$$\Delta^P(\beta,Q^2)=1-g_M^2\bar{U}^{MM}(\beta,Q^2)-g_P^4C_3^2\bar{U}^{MM}(\beta,Q^2)\bar{U}^{PP}(\beta,Q^2), \quad (3.1)$$

i.e.,

$$\Delta^P[\alpha_P{}^{\mathrm{out}}(Q^2),Q^2]=0. \quad (3.2)$$

Similarly, the output M trajectory is defined by

$$\Delta^M[\alpha_M{}^{\mathrm{out}}(Q^2),Q^2]=0, \quad (3.3)$$

with

$$\Delta^M(\beta,Q^2)=[1-C_1g_M^2\bar{U}^{MM}(\beta,Q^2)][1-g_P{}^4|\bar{U}^{PM}(\beta,Q^2)|^2]-2C_2{}^2g_M{}^2g_P{}^2\bar{U}^{MM}(\beta,Q^2)\{\mathrm{Re}[\sigma^{PM}\bar{U}^{PM}(\beta,Q^2)]+g_P{}^2|\bar{U}^{PM}(\beta,Q^2)|^2\}. \quad (3.4)$$

If we define

$$\rho_{P,M}=2\alpha_{P,M}'/a,$$

we have

$$\rho_{P,M}{}^{\mathrm{out}}=-\frac{1}{2}\frac{\partial\Delta^{P,M}(\beta,Q^2)}{\partial(aQ^2)}\Bigg/\frac{\partial\Delta^{P,M}(\beta,Q^2)}{\partial\beta}\Bigg|_{Q^2=0,\ \beta=\alpha_{P,M}{}^{\mathrm{out}}}. \quad (3.5)$$

The output values of ρ and of the trajectory intercepts depend on the input values of ρ, but not on the input slopes and on a separately. Therefore, the independent parameters in the model are α_P, α_M, ρ_P, ρ_M, the coupling constants g_M and g_P, and the model-dependent crossing coefficients C_1, C_2, and C_3. The self-consistency equations $\alpha_{P,M}{}^{\mathrm{out}}=\alpha_{P,M}$ and $\rho_{P,M}{}^{\mathrm{out}}=\rho_{P,M}$ impose four constraints on these parameters.

IV. DOMINANT-P-EXCHANGE LIMIT

In I we presented a model which only includes the interactions (a) and (d) of Fig. 3, i.e., in which only M exchange is present. Now we can put $g_M=0$ and explore the opposite limit, in which only the interactions (c) and (e) of Fig. 3 are left. We observe that in this limit the P trajectory is generated by the iteration of the box diagram of Fig. 4(a), which is equivalent, after a loop integration, to the diagram of Fig. 4(b). This

TABLE I. Solution for dominant-P-exchange model ($g_M=0$) with a meson of isospin 1 ($I_M=1$).

α_M	α_P	g_P^2	ρ_P	ρ_M
0.4	0.78	0.43	0.30	0.29
0.5	0.83	0.35	0.29	0.26
0.6	0.86	0.28	0.26	0.22

gives rise to multi-P-exchange ladders, and with this in mind, we call the $g_M=0$ limit the dominant-P-exchange limit.

It is clear that in this limit the values of C_1 and C_2 are irrelevant. If we assume that the M pole has isospin 1, then $C_3^2=3$. There is only one degree of freedom left, and we can study the solution of the self-consistent equations as a function of α_M. The results are presented in Table I for $\alpha_M=0.4$, 0.5, and 0.6. We observe that the P intercept is too far from 1, and, correspondingly, g_P^2 is much too large.[7] Alternatively, we can let C_3^2 vary as a free parameter and fix α_M—for instance, at $\alpha_M=0.5$. The results in Table II show that it is possible to obtain an intercept for the P pole close to 1, and a small value for g_P^2, but as we approach a solution of this type, C_3^2 increases to values of the order of $1/(1-\alpha_P)=1/\epsilon$, which are difficult to justify. The values of ρ_P and ρ_M are of order ϵ, and the M slope turns out to be smaller than the P slope.

The necessity of having

$$C_3^2\sim 1/\epsilon\sim 1/g_P^2, \tag{4.1}$$

in order to find a solution with ϵ small and $g_M=0$, can be understood if we accept the result

$$\rho_P\sim\rho_M\sim\epsilon \tag{4.2}$$

and examine the espression

$$\bar{U}^{ij}(\beta,0)=v^{ij}(\beta,0)$$
$$=\frac{2}{\rho_i+\rho_j}\Psi\left(1,1,\frac{2}{\rho_i+\rho_j}(\beta-\alpha_i-\alpha_j+1)\right), \tag{4.3}$$

keeping in mind that

$$\lim_{\epsilon\to 0}(1/\epsilon)\Psi(1,1,1/\epsilon)=1. \tag{4.4}$$

TABLE II. Solution for dominant-P-exchange model ($g_M=0$) for $\alpha_M=0.5$ and variable C_3.

α_P	C_3^2	g_P^2	ρ_P	ρ_M
0.999	412	0.0027	0.0040	0.0026
0.99	40.5	0.027	0.038	0.026
0.97	15.6	0.076	0.096	0.069
0.95	9.6	0.11	0.13	0.10
0.91	4.2	0.20	0.21	0.17

[7] See Ref. 2 for a rough phenomenological estimate of g_P^2. Notice that we use $C_3g_P^2$ for what is called g_P^2 in Ref. 2.

We find

$$\bar{U}^{MM}(\alpha_P{}^{\text{out}},0)\sim 1,$$
$$\bar{U}^{PP}(\alpha_P{}^{\text{out}},0)\sim 1/\epsilon, \tag{4.5}$$
$$\bar{U}^{PM}(\alpha_M{}^{\text{out}},0)\sim 1/\epsilon,$$

and Eqs. (3.2) and (3.3) read

$$1-g_P{}^4C_3{}^2\bar{U}^{MM}(\alpha_P{}^{\text{out}},0)\bar{U}^{PP}(\alpha_P{}^{\text{out}},0)=0 \tag{4.6}$$

and

$$1-g_P{}^4[\bar{U}^{PM}(\alpha_P{}^{\text{out}},0)]^2=0. \tag{4.7}$$

The result (4.1) immediately follows.

Large values of C_3^2 are clearly unrealistic, and we can avoid them by introducing in the self-consistent model other mechanisms in addition to those considered in this section.

Before abandoning the dominant-P-exchange model, we examine the energy dependence of the average number of particles produced, $\bar{n}(s)$. Utilizing the optical theorem, we can write for the total cross section

$$\sigma^{\text{tot}}(s)\sim(s/m^2)^{\alpha_P{}^{\text{out}}-1}, \tag{4.8}$$

and therefore

$$\bar{n}(s)=\frac{g_P{}^2C_3}{\sigma^{\text{tot}}(s)}\frac{\partial\sigma^{\text{tot}}(s)}{\partial(g_P{}^2C_3)}\sim g_P{}^2C_3\frac{\partial\alpha_P{}^{\text{out}}}{\partial(g_P{}^2C_3)}\ln(s/m^2). \tag{4.9}$$

From Eqs. (4.2)–(4.6), we find

$$\frac{\partial\alpha_P{}^{\text{out}}}{\partial(g_P{}^2C_3)}\sim\sqrt{\epsilon}, \tag{4.10}$$

and thus, using Eq. (4.1),

$$\bar{n}(s)\sim\epsilon\ln(s/m^2), \tag{4.11}$$

whereas the observed coefficient for a logarithmic dependence of the multiplicity is of order 1. This is another difficulty that arises in the dominant-P-exchange model.

V. MODEL WITH NONVANISHING g_M

We consider now the case in which all the interactions of Fig. 3 are present. In order to gain some insight, we start again with the assumption that the M pole is a pure $I=1$ state. In this case, we have $C_1=\frac{1}{2}$, $C_2{}^2=1$, and $C_3{}^2=3$. We have still two degrees of freedom, which we reduce to one by choosing $\alpha_M=0.5$. We then study the solution as a function of $g_P{}^2$ in the range between the value $g_P{}^2=0.35$ of Table I and $g_P{}^2=0$. The decrease in

TABLE III. Solution for $\alpha_M=0.5$ and $I_M=1$.

α_P	$g_M{}^2$	$g_P{}^2$	ρ_P	ρ_M
0.97	1.18	0.009	0.39	0.26
0.98	1.17	0.006	0.37	0.23
0.99	1.15	0.004	0.35	0.19

g_P^2 is compensated by the effect of a nonvanishing g_M^2. As we can see from Fig. 5, small values of ϵ can be obtained only for small g_P^2, and, correspondingly, g_M^2 of order 1. For instance, if we require $\epsilon<0.03$, we obtain $g_P^2<0.01$.[7]

Some typical solutions are shown in Table III. The small values of g_P^2 obtained suggest that in the interesting range of values of ϵ, the dominant mechanism is M exchange. This exchange gives rise to the terms $C_1 g_M^2 \times \bar{U}^{MM}$ and $g_M^2 \bar{U}^{MM}$ in the determinants Δ^M and Δ^P, respectively, and for $\epsilon=0.03$, these terms account for 80% and more than 99% of the contributions needed to produce the zeros of the respective determinants. The smallness of g_P^2 also makes it possible to neglect the terms of order g_P^4 in Δ^M and Δ^P for $\epsilon<0.03$ without changing the results by more than 2%. This corresponds to neglecting the diagrams (c) and (e) of Fig. 3. If this is done, only the C_1 crossing parameter is relevant, because C_2 merely redefines g_P. We can then relax the assumption of $I=1$ for the meson, and let C_1 vary in some range around the value $\frac{1}{2}$. Table IV shows the results of putting C_1 equal to 0.4 and 0.6. In the limit of $g_P^2=0$, the last case coincides with the model of I.

VI. CONCLUSION

We have investigated the question of how important the P exchange is in a multiperipheral bootstrap model. We had shown in I that a self-consistent solution in which there is no P exchange can be found. Here we began by studying the opposite limit, i.e., the dominant-P-exchange solutions, and found that they are uninteresting, because either the P intercept is too low or unrealistic values of the crossing coefficient C_3 are needed. It is still true in these solutions that the P slope is not smaller than the M slope. In the more general case in which all the interactions of Fig. 3 are present, we conclude that to obtain a P intercept near 1, not only g_P^2 has to be small, but also g_M^2 has to be of order 1. The only significant correction to the M-exchange model arises from the interaction of Fig. 3(b). The main features of the dominant-M-exchange solutions are still present, and again the P slope is of the same order of magnitude as the M slope.

Actually, the P slope obtained is systematically larger than the M slope. The origin of this higher slope can be understood by the following chain of arguments: The contributions of various multiplicities to ImA as a function of t have widths that decrease with n. The average value of n is roughly $\bar{n}=g^2\ln(s/m^2)$. As $\ln(s/m^2)$ increases, the peak of ImA shrinks, because higher values of n dominate. This logarithmic shrinkage is a typical manifestation of Regge behavior. Thus, the output slope originates from the rate at which higher n values become more important.[8] This rate is again roughly proportional to g^2, and therefore it is highest for the vacuum-exchange amplitude.

We do not know how much this result may be altered by more realistic versions and further refinements of the multi-Regge model; it seems unlikely, however, that the multiperipheral bootstrap may produce a P slope significantly smaller than the typical meson slope.

TABLE IV. Solution for $\alpha_M=0.5$ and variable C_1.

C_1	α_P	g_M^2	g_P^2	ρ_P	ρ_M
0.4	0.97	1.14	0.017	0.33	0.20
0.4	0.99	1.11	0.009	0.30	0.13
0.6	0.97	1.28	0.0012	0.49	0.40
0.6	0.99	1.31	0.0002	0.49	0.41

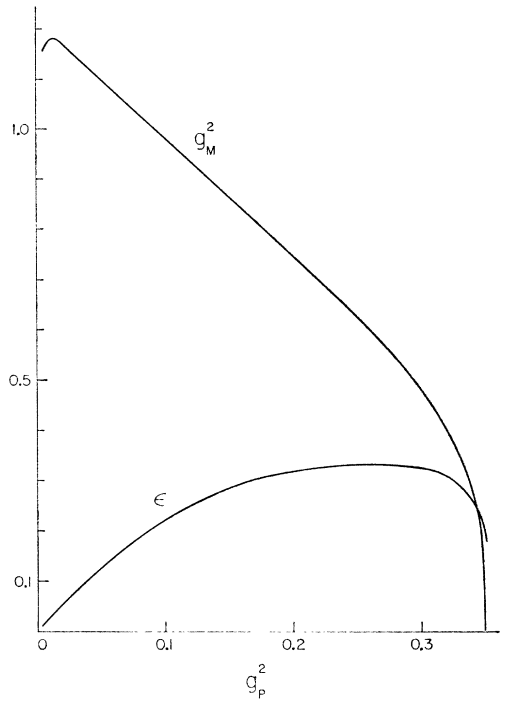

FIG. 5. Dependence of g_M^2 and ϵ on g_P^2 in the model with an M pole of $\alpha_M=0.5$ and isospin 1.

ACKNOWLEDGMENTS

One of the authors (A. P.) wants to acknowledge numerous discussions on subjects related to the present work with Geoffrey Chew, Carleton de Tar, and Peter Ting.

[8] There is another source of output slope in our formalism, because of the shrinkage of the contribution of a fixed multiplicity. This slope is of the cut type, i.e., $\alpha'^{\text{out}}=\frac{1}{2}\alpha'$. It is clear that this mechanism is not sufficient to produce a self-consistent slope different from zero.